JACS
JOURNAL OF THE AMERICAN CHEMICAL SOCIETY
pubs.acs.org/JACS
Article

DNA Electrochemistry: Charge-Transport Pathways through DNA Films on Gold

Adela Nano, Ariel L. Furst,* Michael G. Hill,* and Jacqueline K. Barton*

Cite This: J. Am. Chem. Soc. 2021, 143, 11631−11640
Read Online
ACCESS | Metrics & More | Article Recommendations

ABSTRACT: Over the past 25 years, collective evidence has demonstrated that the DNA base-pair stack serves as a medium for charge transport chemistry in solution and on DNA-modified gold surfaces. Since this charge transport depends sensitively upon the integrity of the DNA base pair stack, perturbations in base stacking, as may occur with DNA base mismatches, lesions, and protein binding, interrupt DNA charge transport (DNA CT). This sensitivity has led to the development of powerful DNA electrochemical sensors. Given the utility of DNA electrochemistry for sensing and in response to recent literature, we describe critical protocols and characterizations necessary for performing DNA-mediated electrochemistry. We demonstrate DNA electrochemistry with a fully AT DNA sequence using a thiolated preformed DNA duplex and distinguish this DNA-mediated chemistry from that of electrochemistry of largely single-stranded DNA adsorbed to the surface. We also demonstrate the dependence of DNA CT on a fully stacked duplex. An increase in the percentage of mismatches within the DNA monolayer leads to a linear decrease in current flow for a DNA-bound intercalator, where the reaction is DNA-mediated; in contrast, for ruthenium hexammine, which binds electrostatically to DNA and the redox chemistry is not DNA-mediated, there is no effect on current flow with mismatches. We find that, with DNA as a well hybridized duplex, upon assembly, a DNA-mediated pathway facilitates the electron transfer between a well coupled redox probe and the gold surface. Overall, this report highlights critical points to be emphasized when utilizing DNA electrochemistry and offers explanations and controls for analyzing confounding results.

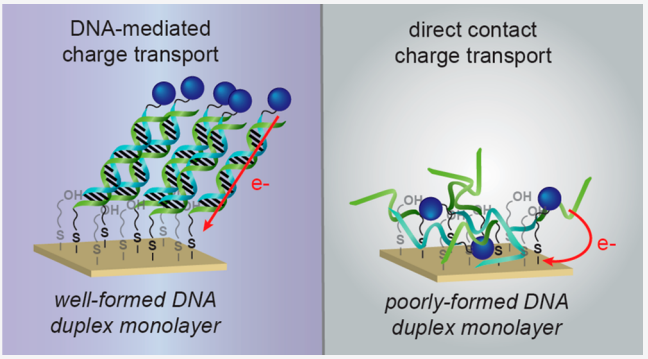

INTRODUCTION

In 1997 we reported that methylene blue (MB) undergoes rapid and efficient electrochemical reduction through close-packed DNA duplexes self-assembled onto gold electrodes via alkylthiol linkers.[1] Subsequent studies with redox probes intercalated site-specifically into the individual helices established that the electrochemical response is independent of the location of the redox probe along the duplex,[2] while the rate of charge transport is limited by the length of the insulating linker as opposed to the DNA, dropping exponentially upon addition of methyl units to the alkylthiol linker.[3] Strikingly, the presence of intervening mismatched bases,[4] abasic sites,[5,6] DNA-binding proteins,[7] and common DNA lesions[8] (e.g., 8-oxo-guanine) attenuates the electrochemical signals, often with "on/off" sensitivity. Electrochemical assays exploiting this signaling element subsequently have been developed for applications ranging from mutational profiling,[9,10] to DNA-methylation,[11,12] to the action of chemotherapeutic agents.[2,13]

A great deal of experimental work has been carried out in our laboratories,[3,14] and others,[15−17] to uncover the governing principles that control charge transport (CT) through these assemblies. Conventional electrochemical methods, (e.g., cyclic voltammetry,[18] chronocoulometry,[19] rotated-disk voltammetry,[20,21] electrochemical impedance spectroscopy[22] etc.,) have been applied to surfaces that have been thoroughly characterized via scanning-probe microscopy (i.e., scanning tunneling microscopy (STM),[23−25] atomic force microscopy (AFM),[26−30] scanning electrochemical microscopy (SECM),[31−33] and spectroscopy (Fourier-transform infrared spectroscopy (FTIR), linear and circular dichroism)).[34] These studies have identified several critical features that impact electrochemical processes at DNA-modified surfaces: (i) small-molecule redox probes can exhibit varied (and sometimes multiple) binding modes to the DNA films, including intercalation, groove binding, and ion pairing, with the mode of binding often depending upon concentration, DNA surface

Received: May 6, 2021
Published: July 26, 2021

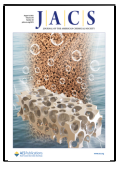

https://doi.org/10.1021/jacs.1c04713
J. Am. Chem. Soc. 2021, 143, 11631−11640

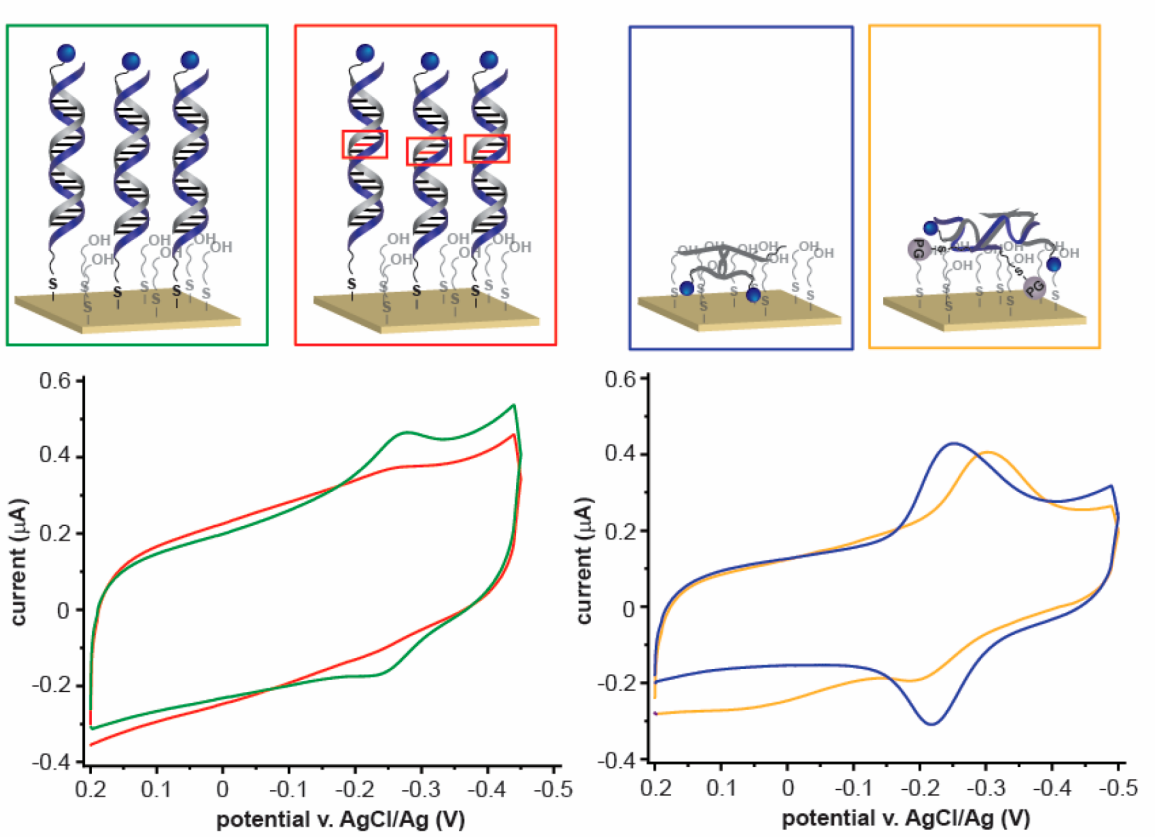

Figure 1. Electrochemistry at all-AT 40-mer DNA sequences. Left: cyclic voltammetry of MB-dsDNA well-matched sequences (in green), and MB-dsDNA sequences containing a single AC mismatch (red). Right: cyclic voltammetry of MB-ssDNA deposited on the gold surface, 5′-MB-AA TAA AAA ATA AAA TAA AAT AAA AAT AAA TAA AAA ATA AT-3′ (blue), and cyclic voltammetry after addition of its complementary strand thiol (PG) protected, 5′-PG-AT TAT TTT TTA TTT ATT TTT ATT TTA TTT TAT TTT TTA TT-3′ (orange). Methylene blue is depicted as a blue sphere connected to the DNA strand. Voltammograms were collected in buffered solutions (5 mM NaH_2PO_3, 50 mM NaCl, pH 7.0), at 100 mV/s scan rate.

density, and the ionic strength of the surrounding electrolyte; (ii) for efficient, long-range CT, the redox probes must be well coupled into the π-stack of DNA; and (iii) the observation of electrochemical signal loss in response to intervening helical π-stack disruptions is a critical and necessary condition for establishing that a process is DNA-mediated.

Despite more than two decades of experimental work, we still do not understand fully the mechanism of DNA-mediated electrochemistry. Early proposals focused on bridge-mediated super exchange and hole hopping, but in each case, the relevant energy gaps are too high to support efficient electrochemical reactions.[35] More recent work has focused on resonance "flickering",[17] or coherent tunneling along electric-field induced delocalized DNA states, providing a theoretical underpinning to understand some key features of DNA-mediated electrochemistry.[36] Very recently, Dauphin-Ducharme, Arroyo-Currás, and Plaxco suggested that electrochemistry on DNA-modified surfaces is not DNA-mediated at all, rather that the electrochemical signals arise from dynamic motions of individual DNA helices that bring redox probes into direct contact with the electrode surface.[37]

Although we investigated that possibility more than two decades ago,[2] this recent report[37] serves to underscore the importance of appropriate and carefully designed control experiments as well as proper surface characterization to generate experimental results that can be reliably interpreted. Motivated by this study, we revisit the possibility of a direct-contact pathway for intercalated probes on double-stranded (dsDNA)-modified surfaces, and we present additional experimental evidence, contextualized within the large body of previously published work, that supports the conclusion that our prior DNA electrochemistry experiments are DNA-mediated. Given the potential roles of DNA-mediated CT in artificial constructs (e.g., nanoscale circuitry, electrochemical DNA-based biosensing, as well as biological pathways), it is critically important to challenge experimental data with robust control experiments to provide reliable experimental findings for experimentalists and theoreticians alike. Here, we highlight key control experiments for validating DNA-mediated electrochemistry, and how variabilities in experimental procedures can lead to potentially distorted conclusions.

RESULTS AND DISCUSSION

Electrochemistry of MB on All-AT DNA Strands. In light of early work on guanine-mediated hole hopping in photochemical charge transport through the double helix, one motivation for reexamining the mechanism of electrochemical charge transport was the contention[37] that efficient DNA-mediated electrochemistry had not been documented using sequences that lacked GC base steps. (We note that the first of several such studies on all-AT duplexes was reported more than two decades ago).[2] The recent study by Dauphin-

https://doi.org/10.1021/jacs.1c04713
J. Am. Chem. Soc. 2021, 143, 11631−11640

Ducharme et al. therefore focused on gold surfaces treated with all-AT single-stranded DNA (ssDNA) modified at the respective 5′- and 3′-ends with a commercial alkylthiol linker and covalently tethered MB. Based on (i) a decrease in the heterogeneous redox kinetics of MB reduction after addition of complementary ssDNA and (ii) no discernible difference between the electrochemical responses of electrodes treated with fully matched vs mismatched complements, they concluded that the electrochemical pathway proceeded via direct contact of MB with the electrode surface, rather than a DNA-mediated process. As we detail below, these findings do support a direct-contact pathway for MB reduction in their system, but they cannot be extrapolated generally to electrodes prepared from duplex DNA, and ought not be used as a framework to reinterpret two decades of experimental work carried out on categorically different DNA assemblies.

To contextualize these findings, we prepared two sets of modified electrodes with sequences identical to those used above, with the important difference that MB was conjugated to the 5′ ends of the non-thiolated, complementary strands to avoid oxidation of the thiol via singlet oxygen sensitized by MB.[38] Figure 1 shows the cyclic voltammetry of MB at films assembled from prehybridized duplexes according to our standard fabrication protocols. Using completely complementary duplexes (green trace), MB undergoes a chemically reversible reduction at −0.25 V vs AgCl/Ag. Integrating the signal yields a surface coverage for electrochemically active MB of ∼3 pmol/cm^2 as compared to an overall duplex surface coverage of ∼10 pmol/cm^2 determined by integrating the electrochemical signal of $Ru(NH_3)_6^{3+}$ bound electrostatically (see below). We have shown previously that the fraction of intercalated MB depends strongly on experimental conditions,[38] and Ferapontova and co-workers[34] have demonstrated the preferred groove-binding mode of MB at AT-rich sequences. Thus, the gap between electrochemically active vs total MB on the surface likely reflects the fraction of intercalated vs groove-bound MB under these conditions. Cyclic voltammetry (CV) rate data for MB reduction using the same intervening AT sequences recorded on a multiplexed chip yield a standard rate constant, $k_o = 67 \pm 10$ s^{-1}, that is fully consistent with decades of previous measurements. Most importantly, repeating these CV experiments under identical conditions but with duplexes possessing an intervening CA mismatch results in a nearly complete loss of MB electrochemistry (red trace). This characteristic mismatch effect has been reported by many different groups,[14,39−42] and supports fully a DNA-mediated pathway for the electrochemical reduction of intercalated redox probes.

For the second set of experiments using these sequences, we followed the approach reported by Dauphin-Ducharme et al. by depositing ssDNA onto gold electrodes, followed by treatment with complementary (matched and mismatched) strands, in a putative attempt to form duplexes on the surface. Using these conditions, we obtained cyclic voltammograms (Figure 1, right) that are remarkably similar to their published results. Yet significantly, *our single-stranded DNA sequences did not possess a thiol linker*. Indeed, both MB and single-stranded DNA oligonucleotides are known to undergo direct adsorption onto gold surfaces.[43,44] Thus, the non-specifically adsorbed ssDNA-MB conjugate undergoes a sharp electrochemical reduction (blue trace) presumably owing to MB in direct contact with the gold surface; adding complementary ssDNA (which also lacks a free thiol linker), broadens the electrochemical signal, indicating more heterogeneity in the kinetics which is expected as a result of the variable and locally inhibited access to the gold surface. Cyclic voltammetry yields a standard reduction rate of 150 s^{-1} for the ssDNA surfaces; attempts to measure the heterogeneous rate constant for MB reduction at electrodes treated with matched and mismatched complements were unsuccessful owing to loss of signal following repeated redox cycling. Notably, unlike the first set of experiments performed using dsDNA, the presence of a mismatched base in the complement yielded no mesurable effect on the electrochemical signal.

Neither our data nor the limited experimental results of the Dauphin-Ducharme study allow us to evaluate the actual extent of surface hybridization vs direct surface adsorption of complementary DNA. Thus, we cannot distinguish between their proposed electrochemical pathway for MB reduction in which oscillating DNA dynamics deliver intercalated MB into direct contact with the electrode,[37] or one in which non-specifically adsorbed complementary ssDNA simply impedes MB access to the surface.

Historical Context for DNA-Mediated Electrochemistry. We have published numerous studies over the years offering experimental insight into the structure and composition of self-assembled DNA films on gold surfaces and have consistently found that certain oligonucleotide preparation and assembly conditions are essential for the formation of a well-ordered DNA monolayer, as opposed to a layer of *non-specifically adsorbed oligonucleotides*. The structures of thiolated DNA monolayers on gold are highly dependent on the specific experimental conditions employed during the deposition process and must be characterized fully in order to draw any meaningful conclusions about DNA-mediated electrochemical pathways. For example, methylene blue (MB), one of the most commonly used small-molecule redox reporters in the field, undergoes quasi-reversible electrochemical reduction at virtually any electrode treated with DNA. Yet, depending on the precise experimental conditions, the MB may be intercalated into the π-stack, groove bound, ion paired to single-stranded phosphate groups, or even adsorbed directly onto unmodified domains of the underlying gold surface; the mere observation of an electrochemical signal is insufficient to assert mechanistic claims regarding the pathway of the electron-transfer event. Fortunately, there exists a toolbox of simple, experimentally validated control experiments that can be carried out routinely to assess both DNA surface density and structure, as well as the binding mode of incorporated redox probes.

DNA Surface Modification. Depending upon the specific application, DNA-modified electrodes featuring a range of DNA surface densities from close-packed to very dilute may be employed (Figure 2). For simplicity, early mechanistic work focused on highly concentrated DNA films. Our basic approach to preparing these constructs involves self-assembling thiol-labeled dsDNA duplexes, typically 15−20 base-pairs long, onto electrochemically etched gold electrodes. In order to achieve high surface concentrations of DNA, $MgCl_2$ is added to the deposition solution to screen the backbone charges on the DNA, minimizing electrostatic repulsion between adjacent duplexes during the self-assembly process. Indeed, we note that kinetic measurements of the film formation show an initial rapid phase in which ∼ 1/4 of the duplexes adsorb to the gold surface within several minutes, followed by a much slower process during which the monolayer is filled in.[1] A similar two-

https://doi.org/10.1021/jacs.1c04713
J. Am. Chem. Soc. 2021, 143, 11631−11640

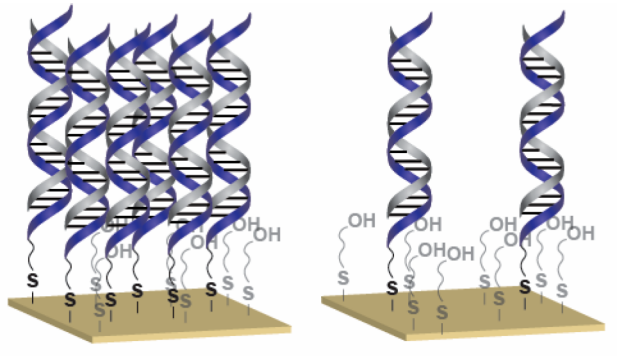

Figure 2. Schematic representation of self-assembled DNA monolayers on the gold surface. Left: densely packed monolayers self-assembled in the presence of $MgCl_2$. Right: loosely packed monolayers self-assembled without $MgCl_2$ and passivated with 6-mercaptohexanol.

dimensional film reconstruction has been proposed for the formation of alkylthiol monolayers.[45−47]

For studies that rely on interactions between bulky components (e.g., proteins) and DNA, lower-density dsDNA monolayers may be required. Notably, we have shown that the uniformity of dilute DNA monolayers is highly dependent on the method of fabrication, and simply reducing the concentration of thiolated dsDNA during the deposition process results in inhomogeneous surfaces.[48,49] Such monolayers are problematic for both characterization and sensing applications. When low-density DNA monolayers are formed through thiol-based self-assembly, the assembly is dominated by inter-helical interactions of adjacent DNA strands. These interactions result in regions of very high DNA density, and other domains with little to no DNA present. Even if the areas without DNA are further passivated with a small molecule such as 6-mercaptohexanol, the inhomogeneity will result in high measurement error and irreproducibility, as disparate regions of the electrode surface will behave differently in response to a stimulus. Thus, to generate uniform low-density monolayers, we first generate a homogeneous, underlying mixed-alkanethiol monolayer,[3] doped with chemically active head groups that enable subsequent DNA bioconjugation to the pre-formed surface.[49] This method of monolayer formation has two key advantages over low-density DNA self-assembled layers: (1) the resulting DNA monolayers are homogeneous, and (2) it enables chemical control over the final density of DNA on the surface, which is key for ensuring efficient interactions between DNA and other biomolecules. We previously showed using AFM that low-density DNA monolayers prepared via attachment of cyclooctyne-modified DNA to mixed monolayers containing active azide head groups form homogeneous layers with only small regions of DNA clustering.[49] Using AFM under fluid conditions, the cluster size was determined and the number of DNA helices present in the cluster calculated. Based on the diameter of the clusters, only ∼50 DNA helices were present in each cluster, which means that the majority of the

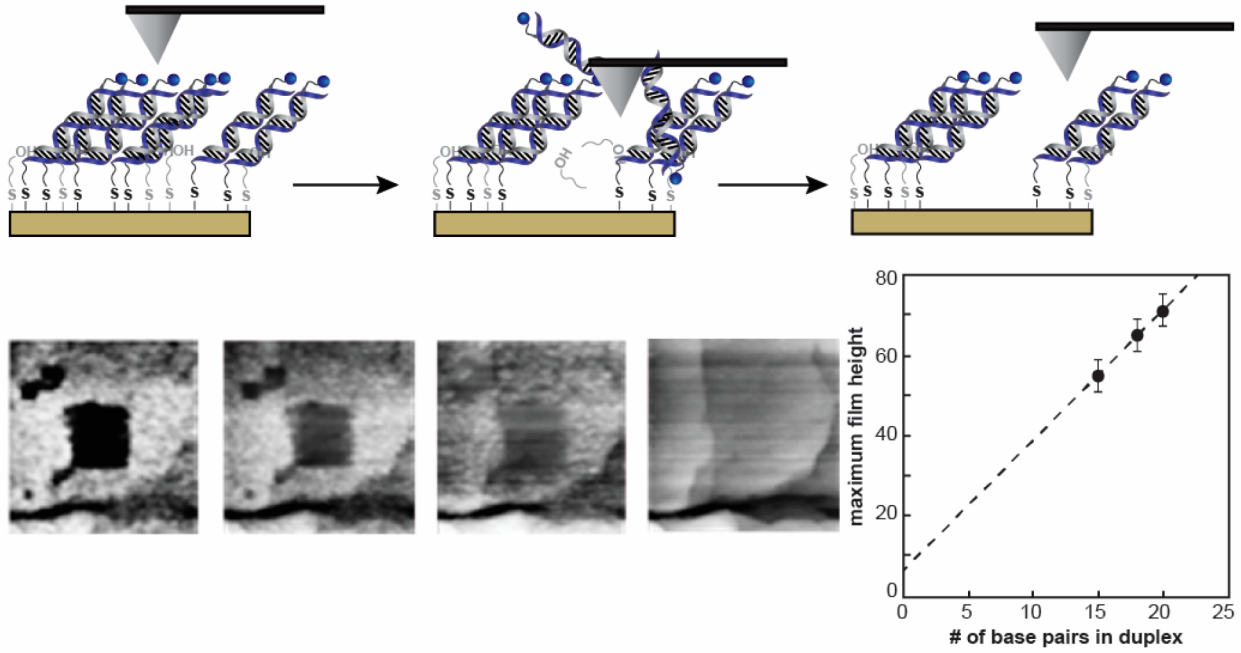

Figure 3. AFM measurement of DNA film height. Upper level: schematic representation showing the height measurement of DNA films. Lower level, left: AFM images (750 nm × 750 nm) of DNA-modified gold (sequence: 5′-SH-AGT ACA GTC ATC GCG-3′) after removal of a small patch (∼100 nm^2) of DNA by mechanically scrapping the probe tip against the surface as indicated by the cartoon representation. The images were recorded under fluid solution (0.1 M potassium phosphate buffer, pH 7), and the height of the DNA was calculated by measuring the depth of the square patch. Moving from left to right are images recorded under electrochemical control as the applied potential was poised negative of the Au/thiol reduction potential; as the thiolated DNA is electrochemically stripped off, the underlying surface features of the gold substrate are revealed. Bottom right: plot of the maximum film height (measured at ∼100 mV vs Ag) measured for MB-DNA duplexes possessing 15 bases (5′-SH-AGT ACA GTC ATC GCG-3′), 18 bases (5′-SH-AGT ACA GTC GTA GTC GCG-3′), and 20 bases (5′-SH-AGT ACA GAT CGT AGC TCG CG-3′). These data show a slope of 3.2 Å/bp, close to the predicted value of 3.4 Å/bp. The intercept, ∼7 Å, is somewhat smaller than the ∼16 Å expected for a fully extended alkylthiol linker, likely due to compression of the film owing to the vertical tip force.

https://doi.org/10.1021/jacs.1c04713
J. Am. Chem. Soc. 2021, 143, 11631−11640

helices are solvent-accessible and therefore present a relatively homogeneous environment.

Characterization of DNA Monolayers. Both high- and low-density films have been characterized extensively via a combination of spectroscopy, electrochemistry, and scanning-probe microscopy.[50] Together, these methods have established several key structural elements of dsDNA monolayers and point to simple electrochemical control experiments that are crucial for subsequent mechanistic work. Below we highlight key structural findings critical for DNA-mediated electrochemistry in these systems, and provide a "road map" for carrying out appropriate control experiments that signal DNA film integrity:

i. Thiolated dsDNA Remains Hybridized during the Self-Assembly Process and Binds to Gold through the Thiol Linker. Direct evidence for the presence of duplexed DNA within these films comes from scintillation counting of surfaces featuring ^{32}P-labeled complements to the thiolated strands.[1,7,51] Likewise, the observation that DNA monolayers are readily stripped from gold (*vide infra*) by applying an electrochemical potential negative of the putative Au(I)-thiolate redox couple indicates that the duplexes are bound to the surface via the thiol linker. Significantly, DNA surface coverages determined by integrating the electrochemical stripping currents yield the same values (~40−50 pmol/cm^2) as surface coverages calculated via quantitative ^{32}P tracing.[1] This duplex density corresponds to a two-dimensional structure of hexagonally close-packed duplexes in which the individual helices are lined up at an angle (~45°) with respect to the electrode surface.

ii. Duplexes Are Oriented Normal to the Electrode Surface at the Applied Electrode Potentials Used for Electrochemical Measurements. To assess the ability of duplex DNA to mediate long-range electrochemical reactions, the individual duplexes must not lie down on the electrode surface. Evidence for upright duplexes has been shown using atomic force microscopy (AFM) studies in fluid solution under electrochemical control.[27,28] While bulk AFM images of freshly prepared DNA monolayers revealed densely packed and uniform surfaces, interactions between the probe tip and the DNA duplexes blurred the images, making it difficult to determine the underlying structures. The orientation of individual DNA duplexes may be assayed by scraping off a small patch of DNA from the monolayer with the AFM tip and then re-imaging the surface (Figure 3). Height-contrast measurements between the resulting hole and the film surface yield a direct measurement of the duplex orientation. Consistent with the 2D structure inferred from ^{32}P tracing and thiol-stripping experiments, at open circuit, the helices align at roughly 45° from the gold surface.

Significantly, applying negative potentials causes the film height to increase from its open-circuit value to values in line with fully extended duplex-linker conjugates oriented normal to the gold surface; on the other hand, positive potentials induce a dramatic height drop to a limiting value of ~20 Å (the diameter of duplex DNA).[28] These changes are reversible, and are consistent with a morphology change that is triggered by electrostatic interactions: at voltages negative of the potential of zero charge (pzc), the negatively charged phosphate backbone is repelled from the surface causing the duplexes to stand straight up, while voltages positive of the pzc attract the phosphate groups causing the duplexes to lie down flat. Accordingly, a plot of the maximum film thickness vs the number of base pairs in the DNA duplexes reveals a nearly ideal slope of 3.4 Å/bp, Figure 3. Subsequent AFM[52] and STM data[23,25] have supported a similar DNA-morphology change upon application of small electric fields.

iii. Electrochemical Assays Using $Ru(NH_3)_6^{3+}$ and $Fe(CN)_6^{3-}$ Provide Routine Validation of DNA Surface Composition and Coverage. Clearly radioactive tracing, AFM imaging, and destructive anodic stripping analyses are impractical for routine film screening. Fortunately, simple, non-destructive, *in situ* electrochemical assays can be used as proxies for these more direct methods. Carried out as part of a standard experimental protocol, these methods provide a convenient tool for surveying the integrity of DNA films before use. For example, Tarlov and Steele have developed a "phosphate-counting" assay for determining the density of nucleic acids on electrode surfaces based on the chronocoulometry of $Ru(NH_3)_6^{3+}$ bound electrostatically to DNA-modified electrodes.[19] Likewise, Yu and co-workers used integrated cyclic voltammetric traces of electrostatically bound $Ru(NH_3)_6^{3+}$ to report on the quantity of both ss- and dsDNA-modified electrodes.[18] These simple assays provide a quick electrochemical alternative to ^{32}P labeling and/or reductive stripping analysis to determine the hybridization state and surface concentration of DNA. It is important to note, however, that significantly changing protocols for film formation, such as utilizing single stranded DNA versus DNA duplexes, requires full characterization of the electrode surface.

We have also developed a complementary approach for examining DNA composition based on long-range electrostatic repulsion of $Fe(CN)_6^{3-/4-}$ from DNA-modified surfaces.[22] This technique uses electrochemical impedance spectroscopy (EIS) to monitor the amount of interfacial resistance (charge transfer resistance, R_{CT}) upon addition of ferri-/ferrocyanide to the solution. As double-stranded DNA not only increases the thickness of the DNA film but also its overall charge, the R_{CT} of such films differs significantly from those assembled with only single-stranded oligonucleotides. For highly precise measurements, establishing the interfacial ionic equilibria required for maintaining charge neutrality within the DNA films can be complicated by $Ru(NH_3)_6^{3+}$, which may participate in equilibria during a faradaic process where mobile cations must cross the film/solution interface to balance charge within the monolayer. The degree to which $Fe(CN)_6^{3-/4-}$ penetrates the film is reflected in the measured impedance arc, providing a quantitative measure of the relative DNA surface coverage. The EIS method has been applied to assay hybridization/dehybridization events of both pure DNA films as well as DNA/mercaptohexanol mixed monolayers. It has proven to be a simple and reliable technique to report on the composition of DNA films under a wide range of experimental conditions; when only qualitative data are needed, the surface coverage of DNA can be quickly screened by noting the degree of $Fe(CN)_6^{3-/4-}$ signal blocking caused by the monolayers.

iv. Hybridization Efficiency Is Highly Dependent on Experimental Conditions. These electrochemical assays have shed light onto the probe/target DNA hybridization process.[43] Very low surface coverages of DNA are required for high hybridization yields; surface coverage values larger than a few pmol/cm^2 evidently impede the capture of target sequences, such that only a small percentage of immobilized probe sequences bind to the complement. The large negative charge density at the DNA-modified surface results in a significant

https://doi.org/10.1021/jacs.1c04713
J. Am. Chem. Soc. 2021, 143, 11631−11640

electrostatic barrier to duplex formation, a factor not encountered in analogous solution-phase processes. Complementary spectroscopic studies have also helped to elaborate the factors controlling hybridization at DNA-modified surfaces.[53−55] Surface-plasmon resonance has been used to monitor DNA target capture in real time and has confirmed that the efficiency of hybridization is maximized at surfaces sparsely covered with probe oligonucleotides.[54,55] This technique was also used to monitor the effects of applied electric fields on hybridization and dehybridization; not surprisingly, it was found that even small fields can significantly accelerate these processes. Mismatched sequences were particularly susceptible to potential-induced dehybridization, an effect that is useful for discriminating between closely related sequences. As similar electric fields are involved in electrochemical assays, the effects of these fields on the DNA-film structure must be considered in the design and interpretation of DNA detection experiments.

Given these considerations, for applications that require surface hybridization of DNA, we have found that the more reliable approach is first to self-assemble thiolated DNA duplexes (vs ssDNA sequences), followed by dehybridization of the resulting sequences to yield ssDNA monolayers suitable for complementary strand capture. Indeed, we used this strategy, coupled to a bioconjugation/electrochemical grafting method,[56] to pattern multiple sequences of dsDNA onto a single electrode surface for use as DNA hybridization probes. Significantly, the ability to encode specific sequences at precise locations on a single electrode enabled the incorporation of both control and experimental sequences on the same surface; using this method, we carried out multiple rounds of hybridization/dehybridization, essentially converting well-matched dsDNA to mismatched dsDNA, and *vice versa*.

v. Signal Attenuation from Single-Base Mismatches or Other π-Stack Lesions Is a Characteristic and Necessary Feature of DNA-Mediated Electrochemistry. While an upright orientation of duplexes within the bulk monolayer is a necessary condition for DNA-mediated processes, it is not sufficient. As noted by Dauphin-Ducharme et al., dynamic motions of the individual helices may transiently deliver redox probes directly onto the electrode surface, where the redox reaction then occurs via a contact-mediated pathway. Indeed, we tested this very possibility in 1999 when we published the first report featuring primarily AT dsDNA films, using covalent daunomycin (DM) bound site specifically as the redox probe.[2] In these assemblies, intercalated DM was cross-linked to a single guanine residue in an otherwise all-AT sequence via the 2-amino group, following previous reports in the literature.[57] Notably, AFM measurements, ^{32}P labeling, and thiol-stripping analyses of both fully complementary and mismatched sequences all confirmed that the DNA surface density and overall film structure were indistinguishable from monolayers comprised of duplexes not labeled with DM. As we reported, efficient electrochemical reduction of DM occurred regardless of its position along the ∼45-Å-long, 15-base-pair sequence, yet *a single intervening CA mismatch switched off the electrochemical response entirely*.

This mismatch effect offers a convenient handle to validate a through-helical (vs contact-mediated) pathway for electrochemical reduction of intercalated probes. For example, Figure 4 summarizes the experimental results obtained from experiments carried out on a series of DM-labeled dsDNA monolayers prepared from deposition solutions containing

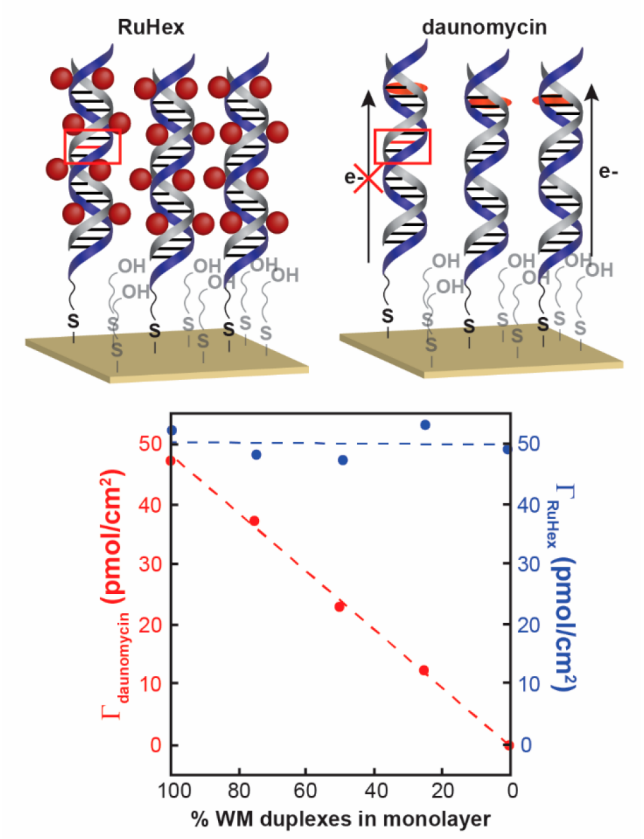

Figure 4. $Ru(NH_3)_6^{3+}$ vs daunomycin interaction with duplex DNA. $Ru(NH_3)_6^{3+}$ (RuHex) complexes bind to DNA electrostatically and are generally not sequence-specific. Since the binding is to the phosphates, the electrochemistry is not expected to be DNA-mediated, and the electrochemical readout from RuHex does not change in the presence of a mismatch site in the duplex DNA. As seen in the plot, the surface concentration of bound $Ru(NH_3)_6^{3+}$ (Γ_{Ru}, mol/cm^2) in the DNA film with varying % of well-matched (WM) duplexes remains constant. In contrast, a mismatch perturbation switches off the signal from the covalently bound DNA intercalator daunomycin. Consequently, the readout of surface concentration of bound daunomycin ($\Gamma_{daunomycin}$, mol/cm^2) decreases linearly with decreasing % of well-matched dsDNA in the monolayer. The DNA sequence is 5′-SH-ATC CTC AAT CAT **GG**A C-3′, where **GG** represents the daunomycin cross-linking site and *C* represents the site of an AC mismatch for mismatched duplexes.

various mole fractions of mismatched DM-labeled duplexes. The total number of DM-labeled duplexes on the surface was determined by $Ru(NH_3)_6^{3+}$-based phosphate counting, while the integrated DM reduction signals provided a direct measure of the fraction of the labeled duplexes that were electrochemically active. As illustrated in the coulometric data, the DM reduction signals drop linearly with increasing mole fractions of mismatched duplexes, even though the total number of DM-labeled duplexes (matched plus mismatched) on the surface remains constant. These results not only preclude a contact-mediated mechanism gated by DNA helical dynamics, but also eliminate a related pathway in which electron transfer occurs at defect "hot spots" within the film, followed by lateral diffusion of DM reduction throughout the monolayer.

Subsequent work has demonstrated this same mismatch effect at dsDNA modified surfaces using GC-rich sequences, AT-rich sequences, and duplexes containing each of the

https://doi.org/10.1021/jacs.1c04713
J. Am. Chem. Soc. 2021, 143, 11631−11640

possible single-base mismatches.[58] Indeed, helix-disrupting DNA lesions[8] and protein-binding events that kink the helical structure[59,60] cause a similar attenuation of electrochemical signals. It is a characteristic feature of dsDNA films that disruption of π-stack primarily affects the yield of charge transfer (as opposed to the *rate* of charge transfer) further implicating a DNA-mediated pathway for the redox reactions of intercalated probes.

Reevaluating the Rationale for a Contact-Mediated Electrochemical Pathway. Within the context of our current results, as well as the extensive body of work highlighted above, it is clear that films prepared from ssDNA sequences are categorically different from films prepared from dsDNA. In this light, it is instructive to revisit the specific arguments that Dauphin-Ducharme et al. invoke to conclude broadly that DNA-based electrochemistry is dominated by contact-mediated pathways.

Their first claim is that the DNA-mediated community cites hole-hopping through guanine bases as a necessary condition of DNA-mediated electrochemistry. It is true that various mechanistic proposals, including hole-hopping between guanine sites in *photochemical* DNA CT, fueled our early investigations of the effect of base composition and sequence on long-range, photoinduced oxidative DNA damage.[15,16,61−63] However, the DNA electrochemistry community has not invoked a guanine hole-hopping mechanism for electrochemical *reduction* of intercalated probe molecules. Indeed, Ferapontova and co-workers have carried out detailed experiments featuring AT, GC, and mixed DNA sequences, in which they report DNA-mediated electrochemistry for bound MB at low packing densities using a thiolated 25-mer all-AT sequence, a 20-mer all-GC sequence, and a mixed-composition sequence.[34] Their work shows convincingly that the mode of interaction of MB with AT sequences depends upon ionic strength, while establishing conditions for intercalation vs groove binding at AT and GC sequences. They additionally report detailed electrode kinetics showing that electron transfer rates for groove-bound MB are greater than rates for intercalated MB. These and other published studies show explicitly that a guanine-hopping model cannot account for charge transport in DNA-mediated electrochemistry.

A second claim of the Dauphin-Ducharme study[37] is that heterogeneous rate constants determined via chronoamperometry are superior to analogous rate constants measured via cyclic voltammetry. Chronoamperometry has been used effectively to measure electrochemical ET rates of redox probes attached to self-assembled monolayers on gold,[64,65] but there are important considerations to bear in mind when using this technique: (i) iR drop must be carefully controlled, as the exponential decrease in current during the measurement cycle necessarily results in an analogous drop in the applied electrochemical potential, and (ii) the ET rate constant itself is dependent on the electrochemical overpotential. Thus, it is important to record chronoamperometry traces as a function of applied potential so that rates from different systems can be accurately compared at the same thermodynamic driving force, usually at zero driving force. Neither of these issues appear to have been accounted for in the Dauphin-Ducharme study. Clearly, these same factors also apply when measuring rates via cyclic voltammetry, yet those measurements yield the zero-overpotential rate constants directly, facilitating comparisons between different systems. We note that Bond has written extensively about the heuristic nature of Laviron's cyclic voltammetry method, and has proposed an alternative procedure based upon AC voltammetry for more accurately measuring rate constants.[66] In the absence of these types of data, we have been very conservative in reporting the precision of our cyclic-voltammetry-measured rate constants; indeed, the actual rates are of secondary importance, as the fact that there is a signal at all supports rapid electron transfer.

A third factor cited in the Dauphin-Ducharme study in support of a general contact-mediated pathway involves a supposition about the hybridization state of DNA on the surface. The authors speculate that forming monolayers from dsDNA leads to partial dehybridization, resulting in surfaces contaminated with ssDNA, thus precluding a DNA-mediated electrochemical pathway. This speculation is inconsistent with many empirical findings (e.g., ^{32}P tracing, AFM imaging, phosphate counting, impedance spectroscopy, surface IR and CD spectroscopy, and mismatch-doping experiments, cf. Figure 4). Notably, surface dehybridization cannot account for the dramatic signal attenuation caused by mismatches and other π-stack lesions that characterizes electrochemistry at dsDNA- but not ssDNA-modified surfaces.

Finally, and perhaps most importantly, we note that the experimental procedures reported by Dauphin-Ducharme[37] for monolayer assembly very likely yield non-specifically adsorbed single-stranded oligonucleotides. For example, Dauphin-Ducharme et al. incubate unusually low concentrations (0.2−3 μM) of single-stranded DNA on gold for just 1 h, compared to the overnight self-assembly of thiolated duplexes (10−100 μM) typically employed by us. Moreover, the Dauphin-Ducharme protocol involves subsequent electrode passivation by treating the ssDNA-modified electrodes with 6-mercapto-hexanol (MCH) overnight. In contrast, we typically treat dsDNA-modified electrodes with MCH for 10−45 min. Indeed, overnight MCH incubation raises questions about the integrity of the Dauphin-Ducharme monolayers.[37] There is robust data in the literature[67,68] establishing the ability of MCH to displace thiol-immobilized DNA on gold. Lee et al. find that ∼0.5−1 h MCH exposure leads to a maximum disruption of the weaker, non-specific interactions between nitrogen-containing nucleobases and gold, presumably promoting reorientation of the ssDNA oligomers in a more upright position. Longer incubation time, however, may favor DNA displacement from the gold surface. Although the nature of the underlying surface composition of their monolayers remains unknown, Dauphin-Ducharme et al. present chronoamperometry data that indicate a change in the current decay upon addition of 100 nM complement to their electrodes; while this change is attributed to surface hybridization, no supporting structural data is presented, nor does the observation that the process is complete within 5 min suggest discrete hybridization, given the challenges of surface hybridization noted above.

An additional complicating factor involves the conditions used for reduction of the terminal disulfide of their labeled sequence prior to deposition.[37] In order to achieve full deprotection, we treat the disulfide-protected sequences with 50 equiv of TCEP in NaP_i buffer (pH 7.5), monitoring the reaction via HPLC. Quantitative UV−vis measurements using Ellman's assay for free thiol[69] show that under these conditions, a 1 h reaction does not lead to a complete thiol deprotection; 2.5−3 h are required to achieve full thiol deprotection at ambient temperature. Thus, with all of these

https://doi.org/10.1021/jacs.1c04713
J. Am. Chem. Soc. 2021, 143, 11631−11640

unresolved questions surrounding the Dauphin-Ducharme protocol for electrode modification, it is more likely that the electrodes utilized in their report have non-specifically adsorbed single-stranded DNA sequences that enable direct interaction of the MB redox probe with the electrode surface, similar to the constructs that we prepared from non-thiolated ssDNA, +/− complement, shown in Figure 1.

CONCLUSIONS

DNA-mediated electrochemistry represents a powerful method for sensing DNA integrity and the binding and/or reaction of proteins with the DNA duplex. For this technology to be meaningfully applied, DNA films must be fully characterized, controls included, and protocols followed, to ensure that the electrochemistry is indeed DNA-mediated, and thus a sensitive monitor of the integrity of the intervening duplex. Here we show DNA-mediated electrochemistry with a fully AT DNA sequence using a thiolated preformed DNA duplex and its contrast to electrochemistry of largely single-stranded DNA adsorbed to the surface. For DNA-mediated redox chemistry to be detected effectively, the duplex must be bound in a manner normal to the surface, as we show. Of critical importance is establishing that the redox chemistry is DNA-mediated for a given DNA monolayer. Most convenient is assessing the DNA mediation through showing that an intervening mismatch or other helical perturbation interrupts the redox process. DNA-mediated electrochemistry depends critically on the DNA monolayer, and indeed when the monolayer is not well characterized and protocols not followed, alternative pathways for reaction of a redox probe bound to the surface become available. However, if the redox reaction of the DNA-bound redox probe is to be a reporter of the integrity of the DNA helix, the redox reaction must occur through the DNA base paired stack. Our mechanistic understanding of this ground state electron transfer process is not well established currently and requires more theoretical study. However, it is increasingly clear that ground state electron transfer through the DNA base pair stack is utilized by Nature and can also be sensitively utilized in well characterized experiments for DNA sensing.

EXPERIMENTAL METHODS

Materials. Tris(2-carboxyethyl)phosphine hydrochloride (TCEP) and 6-mercapto-1-hexanol (MCH) were obtained from Sigma-Aldrich and used as received. All the DNA sequences used in this study were purchased from Integrated DNA Technologies. The buffers were prepared using Milli-Q water (>18 MΩ cm).

Oligonucleotide Preparation. The double-stranded MB-DNA sequences used for AFM measurements (5′-AGTACAGTCATCGCG-3′; 5′-AGTACAGTCGTAGTCGCG-3′, and 5′-AGTACAGATCGTAGCTCGCG-3′ along with the corresponding complementary strand covalently linked to MB at 5′-end of the sequence) were prepared as previously published.[28] Similarly, daunomycin-labeled sequences (5′-ATCCTCAATCA**GG**AC-3′, where **GG** represents the binding site, and C represents the site of an AC mismatch) were prepared as reported.[3] The 40-mer DNA sequences (all-AT parent strand: 5′-$(CH_2)_6$SS-AT TAT TTT TTA TTT ATT TTT ATT TTA TTT TAT TTT TTA TT-3′; MB-all-AT complement strand: 5′-MB-AA TAA AAA ATA AAA TAA AAT AAA AAT AAA TAA AAA ATA AT-3′, and MB-allAT mismatched strand 5′-MB-AA TAA AAA ATA AAA TAA AAT AAA AAT ACA TAA AAA ATA AT-3′) were obtained from Integrated DNA Technologies (IDT) and purified by reverse-phase high-pressure liquid chromatography (HP 1100, Agilent) using a C-18 column (PLRP-S, Agilent). After HPLC purification, each strand was characterized using matrix-assisted laser desorption−ionization (MALDI) mass spectrometry. The disulfide bond of thiol-protected strands was reduced with 50 equiv of tris(2-carboxyethyl)phosphine hydrochloride (TCEP) in NaPi buffer (5 mM NaH_2PO_3, 50 mM NaCl, pH 7.0) under aerobic conditions. The reaction mixture was incubated at room temperature with gentle shaking for 3 h, yielding quantitative deprotected thiol-terminal sequence as indicated by analytical HPLC traces. The resulting thiolated oligonucleotides were purified using Micro Bio-Spin chromatography columns (Bio-Rad), which were previously equilibrated with NaP_i buffer. The concentrations of thiolated and respective complementary strands were adjusted to 100 mM using the absorbances at 260 nm, and the corresponding extinction coefficients obtained from IDT. Strands were then combined in equal volumes and the mixtures deoxygenated by bubbling argon for 2 min for every 50 μL. The samples were immediately sealed using parafilm and Teflon tape to avoid evaporation and annealed for 5 min at 90 °C using a thermocycler, followed by slow cooling to room temperature over 90 min. The annealing yielded doublestranded DNA with a final concentration 50 μM. The resulting duplexed strands were stored under strict anaerobic conditions at −20 °C until further use.

DNA Self-Assembled Monolayers Preparation. DNA was immobilized by incubating the clean gold electrodes with 10 μL DNA (50 μM for dsDNA, 1 μM for ssDNA) in NaPi buffer (5 mM NaH_2PO_4, 50 mM NaCl, pH 7.0) overnight in humid environment, and protected from light. After incubation each electrode was rinsed with buffer several times before passivation with MCH.

Electrochemical Measurements. Electrochemical measurements were performed using a three-electrode setup with a DNA-modified Au working electrode, a Pt auxiliary electrode, and a Ag/AgCl reference electrode. Variable scan rate cyclic voltammetry data were collected over a window 0.2 to −0.5 mV versus Ag/AgCl.

Atomic Force Microscopy. All AFM images were collected using a MultiMode atomic force microscope running on the NanoScope IIIa controller (Digital Instruments, Santa Barbara, CA). A glass AFM electrochemistry chamber (Digital Instruments, Santa Barbara, CA) and a fluid volume of approximately 50 μL were used for the experiments. Si_3N_4 cantilevers (spring constant: 0.06 N/m) with integrated, end-mounted, oxide-sharpened Si_3N_4 probe tips were used. The applied vertical force of the AFM probe during imaging was minimized to beneath 200 pN. Continually adjusting the cantilever deflection feedback set point compensated for thermal drifting of the cantilever, and a consistent minimum force was maintained. AFM height calibrations were carried out on a NIST-traceable 180 nm height standard and then confirmed by measuring a single-atom step in the Au surface. The AFM images were recorded in either "Height" (constant force) or tapping mode. Potentials were controlled by a Princeton Applied Research Model 173 potentiostat/galvanostat, using silver and platinum wires for the pseudoreference and auxiliary electrodes, respectively.

AUTHOR INFORMATION

Corresponding Authors

Ariel L. Furst − *Department of Chemical Engineering, Massachusetts Institute of Technology, Cambridge, Massachusetts 02139, United States;* orcid.org/0000-0001-9583-9703; Email: afurst@mit.edu

Michael G. Hill − *Department of Chemistry, Occidental College, Los Angeles, California 90041, United States;* Email: mgh@oxy.edu

Jacqueline K. Barton − *Division of Chemistry and Chemical Engineering, California Institute of Technology, Pasadena, California 91125, United States;* orcid.org/0000-0001-9883-1600; Email: jkbarton@cco.caltech.edu

https://doi.org/10.1021/jacs.1c04713
J. Am. Chem. Soc. 2021, 143, 11631−11640

Author

Adela Nano − *Division of Chemistry and Chemical Engineering, California Institute of Technology, Pasadena, California 91125, United States*

Complete contact information is available at: https://pubs.acs.org/10.1021/jacs.1c04713

Notes

The authors declare no competing financial interest.

■ ACKNOWLEDGMENTS

We are grateful to the NIH (GM126904) for their continued support of this research. We are also grateful to our many collaborators over the years who developed this powerful chemistry, despite some skepticism, and creatively designed new sensor technology.

■ REFERENCES

(1) Kelley, S. O.; Barton, J. K.; Jackson, N. M.; Hill, M. G. Electrochemistry of methylene blue bound to a DNA-modified electrode. *Bioconjugate Chem.* **1997**, *8*, 31−37.

(2) Kelley, S. O.; Jackson, N. M.; Hill, M. G.; Barton, J. K. Long Range Electron Transfer Through DNA Films. *Angew. Chem., Int. Ed.* **1999**, *38*, 941−945.

(3) Drummond, T. G.; Hill, M. G.; Barton, J. K. Electron transfer rates in DNA films as a function of tether length. *J. Am. Chem. Soc.* **2004**, *126*, 15010−15011.

(4) Pheeney, C. G.; Barton, J. K. *Langmuir* **2012**, *28*, 7063−7070.

(5) McWilliams, M. A.; Bhui, R.; Taylor, D. W.; Slinker, J. D. The Electronic Influence of Abasic Sites in DNA. *J. Am. Chem. Soc.* **2015**, *137*, 11150−11155.

(6) Buzzeo, M. C.; Barton, J. K. Redmond Red as a Redox Probe for the DNA-Mediated Detection of Abasic Sites Bioconjug. *Bioconjugate Chem.* **2008**, *19*, 2110−2112.

(7) Boon, E.; Salas, J.; Barton, J. An electrical probe of protein−DNA interactions on DNA-modified surfaces. *Nat. Biotechnol.* **2002**, *20*, 282−286.

(8) Boal, A. K.; Barton, J. K. Electrochemical detection of lesions in DNA. *Bioconjugate Chem.* **2005**, *16*, 312−321.

(9) Yang, H.; Hui, A.; Pampalakis, G.; Soleymani, L.; Liu, F. F.; Sargent, E. H.; Kelley, S. O. Direct, electronic microRNA detection for the rapid determination of differential expression profiles. *Angew. Chem., Int. Ed.* **2009**, *48*, 8461−8464.

(10) Boon, E. M.; Ceres, D. M.; Drummond, T. G.; Hill, M. G.; Barton, J. K. Mutation detection by electrocatalysis at DNA-modified electrodes [published correction appears in *Nat. Biotechnol.* **2000**,*18*, 1318]. *Nat. Biotechnol.* **2000**, *18*, 1096−1100.

(11) Wang, G. L.; Zhou, L. Y.; Luo, H. Q.; Li, N. B. Electrochemical strategy for sensing DNA methylation and DNA methyltransferase activity. *Anal. Chim. Acta* **2013**, *768*, 76−81.

(12) Muren, N. B.; Barton, J. K. Electrochemical assay for the signal-on detection of human DNA methyltransferase activity. *J. Am. Chem. Soc.* **2013**, *135*, 16632−16640.

(13) Kahanda, D.; Singh, N.; Boothman, D. A.; Slinker, J. D. Following anticancer drug activity in cell lysates with DNA devices. *Biosens. Bioelectron.* **2018**, *119*, 1−9.

(14) Genereux, J. G.; Barton, J. K. Mechanisms for DNA Charge Transport. *Chem. Rev.* **2010**, *110*, 1642−1662.

(15) Henderson, P. T.; Jones, D.; Hampikian, G.; Kan, Y.; Schuster, G. B. Long-distance charge transport in duplex DNA: The phonon-assisted polaron-like hopping mechanism. *Proc. Natl. Acad. Sci. U. S. A.* **1999**, *96*, 8353−8358.

(16) Conwell, E. M.; Rakhmanova, S. V. Polarons in DNA. *Proc. Natl. Acad. Sci. U. S. A.* **2000**, *97*, 4556−4560.

(17) Zhang, Y.; Liu, C.; Balaeff, A.; Skourtis, S. S.; Beratan, D. N. Biological charge transfer via flickering resonance. *Proc. Natl. Acad. Sci. U. S. A.* **2014**, *111*, 10049−10054.

(18) Yu, H.-Z.; Luo, C.-Y.; Sankar, C. G.; Sen, D. Voltammetric Procedure for Examining DNA-Modified Surfaces: Quantitation, Cationic Binding Activity, and Electron-Transfer Kinetics. *Anal. Chem.* **2003**, *75*, 3902−3907.

(19) Steel, A. B.; Herne, T. M.; Tarlov, M. J. Electrochemical Quantitation of DNA Immobilized on Gold. *Anal. Chem.* **1998**, *70*, 4670−4677.

(20) Bard, A. J.; Faulkner, L. R. *Electrochemical Methods: Fundamentals and Applications*, 2nd ed.; John Wiley & Sons: New York, 2001, pp 30−40.

(21) Boon, E. M.; Barton, J. K.; Bhagat, V.; Nersissian, M.; Wang, W.; Hill, M. G. Reduction of Ferricyanide by Methylene Blue at a DNA-Modified Rotating-Disk Electrode. *Langmuir* **2003**, *19*, 9255−9259.

(22) Ceres, D. M.; Udit, A. K.; Hill, H. D.; Hill, M. G.; Barton, J. K. Differential ionic permeation of DNA-modified electrodes. *J. Phys. Chem. B* **2007**, *111*, 663−668.

(23) Ceres, D. M.; Barton, J. K. In situ scanning tunneling microscopy of DNA-modified gold surfaces: bias and mismatch dependence. *J. Am. Chem. Soc.* **2003**, *125*, 14964−14965.

(24) Hihath, J.; Xu, B.; Zhang, P.; Tao, N. Study of single-nucleotide polymorphisms by means of electrical conductance measurements. *Proc. Natl. Acad. Sci. U. S. A.* **2005**, *102*, 16979−16983.

(25) Wierzbinski, E.; Arndt, J.; Hammond, W.; Slowinski, K. In situ electrochemical distance tunneling spectroscopy of ds-DNA molecules. *Langmuir* **2006**, *22*, 2426−2429.

(26) Gorodetsky, A. A.; Barton, J. K. Electrochemistry using self-assembled DNA monolayers on highly oriented pyrolytic graphite. *Langmuir* **2006**, *22*, 7917−7922.

(27) Boon, E. M.; Barton, J. K.; Sam, M.; Hill, M. G.; Spain, E. M. Morphology of 15-mer duplexes Tethered to Au(111) *via* Atomic and Chemical Force Microscopies. *Langmuir* **2001**, *17*, 5727−5730.

(28) Kelley, S. O.; Barton, J. K.; Jackson, N. M.; McPherson, L. D.; Potter, A. B.; Spain, E. M.; Allen, M. J.; Hill, M. G. Orienting DNA Helices on Gold using Applied Electrice Fields. *Langmuir* **1998**, *14*, 6781−6784.

(29) Zhou, D.; Sinniah, K.; Abell, C.; Rayment, T. Use of Atomic Force Microscopy for Making Addresses in DNA Coatings. *Langmuir* **2002**, *18*, 8278−8281.

(30) Zhou, D.; Sinniah, K.; Abell, C.; Rayment, T. Label Free Detection of DNA Hybridization at the Nanoscale: A Highly Sensitive and Selective Approach Using Atomic-Force Microscopy. *Angew. Chem., Int. Ed.* **2003**, *42*, 4934−4937.

(31) Turcu, F.; Schulte, A.; Hartwich, G.; Schuhmann, W. Label Free Electrochemical Recognition of DNA Hybridization by Means of Modulation of the Feedback Current of SECM. *Angew. Chem., Int. Ed.* **2004**, *43*, 3482−3485.

(32) Liu, B.; Bard, A. J.; Li, C. Z.; Kraatz, H. B. Scanning electrochemical microscopy. 51. Studies of self-assembled monolayers of DNA in the absence and presence of metal ions. *J. Phys. Chem. B* **2005**, *109*, 5193−5198.

(33) Wain, A. J.; Zhou, F. Scanning electrochemical microscopy imaging of DNA microarrays using methylene blue as a redox-active intercalator. *Langmuir* **2008**, *24*, 5155−5160.

(34) Kékedy-Nagy, L.; Ferapontova, E. E. Sequence-Specific Electron Transfer Mediated by DNA Duplexes Attached to Gold through the Alkanethiol Linker. *J. Phys. Chem. B* **2018**, *122*, 10077−10085.

(35) Treadway, C. R.; Hill, M. G.; Barton, J. K. Charge transport through a molecular π-stack: double helical DNA. *Chem. Phys.* **2002**, *281*, 409−428.

(36) Michaeli, K.; Beratan, D. N.; Waldeck, D. H.; Naaman, R. Voltage-induced long-range coherent electron transfer through organic molecules. *Proc. Natl. Acad. Sci. U. S. A.* **2019**, *116*, 5931−5936.

(37) Dauphin-Ducharme, P.; Arroyo-Currás, N.; Plaxco, K. W. High-Precision Electrochemical Measurements of the Guanine-, Mismatch-, and Length-Dependence of Electron Transfer from Electrode-Bound DNA Are Consistent with a Contact-Mediated Mechanism.

[published correction appears in *J. Am. Chem. Soc.* **2019**, *141*, 8000]. *J. Am. Chem. Soc.* **2019**, *141*, 1304−1311.
(38) Boon, E. M.; Jackson, N. M.; Wightman, M. D.; Kelley, S. O.; Hill, M. G.; Barton, J. K. Intercalative Stacking: A Critical Feature of DNA Charge-Transport Electrochemistry. *J. Phys. Chem. B* **2003**, *107*, 11805−11812.
(39) Kékedy-Nagy, L.; Ferapontova, E. E. Directional Preference of DNA-Mediated Electron Transfer in Gold-Tethered DNA Duplexes: Is DNA a Molecular Rectifier? *Angew. Chem., Int. Ed.* **2019**, *58*, 3048−3052.
(40) Hartwich, G.; Caruana, D. J.; de Lumley-Woodyear, T.; Wu, Y.; Campbell, C. N.; Heller, A. Electrochemical Study of Electron Transport through Thin DNA Films. *J. Am. Chem. Soc.* **1999**, *121* (46), 10803−10812.
(41) Lu, N.; Pei, H.; Ge, Z.; Simmons, C. R.; Yan, H.; Fan, C. Charge Transport within a Three-Dimensional DNA Nanostructure Framework. *J. Am. Chem. Soc.* **2012**, *134* (32), 13148−13151.
(42) Wohlgamuth, C. H.; McWilliams, M. A.; Slinker, J. D. DNA as a Molecular Wire: Distance and Sequence Dependence. *Anal. Chem.* **2013**, *85* (18), 8634−8640.
(43) Steel, A. B.; Levicky, R. L.; Herne, T. M.; Tarlov, M. J. Immobilization of Nucleic Acids at Solid Surfaces: Effect of Oligonucleotide Length on Layer Assembly. *Biophys. J.* **2000**, *79*, 975−981.
(44) Song, Y.; Wang, L. Well-ordered structure of methylene blue monolayers on Au(111) surface: electrochemical scanning tunneling microscopy studies. *Microsc. Res. Tech.* **2009**, *72*, 79−84.
(45) Poirier, G. E.; Pylant, E. D. The Self-Assembly Mechanism of Alkanethiols on Au(111). *Science* **1996**, *272*, 1145−1148.
(46) Xu, S.; Liu, G.-Y. Nanometer-Scale Fabrication by Simultaneous Nanoshaving and Molecular self-Assembly. *Langmuir* **1997**, *13*, 127−129.
(47) Xu, S.; Cruchon-Dupeyrat, S. J. N.; Garno, J. C.; Liu, G.-Y.; Jennings, G. K.; Yong, T.-H.; Laibinis, P. E. *In Situ* Studies of Thiol Self-Assembly on Gold from Solution using Atomic force Microscopy. *J. Chem. Phys.* **1998**, *108*, 5002−5012.
(48) Murphy, J. N.; Cheng, A. K. H.; Yu, H.-Z.; Bizzotto, D. On the Nature of DNA Self-Assembled Monolayers on Au: Measuring Surface Heterogeneity with Electrochemical in Situ Fluorescence Microscopy. *J. Am. Chem. Soc.* **2009**, *131* (11), 4042−4050.
(49) Furst, A. L.; Hill, M. G.; Barton, J. K. DNA-modified electrodes fabricated using copper-free click chemistry for enhanced protein detection. *Langmuir* **2013**, *29*, 16141−16149.
(50) Scanning probe microscopy is considered to be a robust technique for accurate height measurement of features on a surface. See, for example: Lillehei, P. T.; Bottomley, L. A. Scanning Probe Microscopy. *Anal. Chem.* **2000**, *72*, 189−196.
(51) Gore, M. R.; Szalai, V. A.; Ropp, P. A.; Yang, I. V.; Silverman, J. S.; Thorp, H. H. Detection of Attomole Quantitites of DNA Targets on Gold Microelectrodes by Electrocatalytic Nucleobase Oxidation. *Anal. Chem.* **2003**, *75*, 6586−6592.
(52) Rant, U.; Arinaga, K.; Fujita, S.; Yokoyama, N.; Abstreiter, G.; Tornow, M. Dynamic Electrical Switching of DNA Layers on a Metal Surface. *Nano Lett.* **2004**, *4*, 2441−2445.
(53) Heaton, R. J.; Peterson, A. W.; Georgiadis, R. M. Electrostatic Surface Plasmon Resonance: Direct Electric Field-Induced Hybridization and Denaturation in Monolayer Nucleic Acid Films and Label-Free Discrimination of Base Mismatches. *Proc. Natl. Acad. Sci. U. S. A.* **2001**, *98*, 3701−3704.
(54) Peterson, A. W.; Heaton, R. J.; Georgiadis, R. M. The Effect of Surface Probe density on DNA Hybridization. *Nucleic Acids Res.* **2001**, *29*, 5163−5168.
(55) Peterson, A. W.; Wolf, L. K.; Georgiadis, R. M. Hybridization of Mismatched or Partially Matched DNA at Surfaces. *J. Am. Chem. Soc.* **2002**, *124*, 14601−14607.
(56) Furst, A. L.; Muren, N. B.; Hill, M. G.; Barton, J. K. Label-free electrochemical detection of human methyltransferase from tumors. *Proc. Natl. Acad. Sci. U. S. A.* **2014**, *111*, 14985−14989.
(57) Wang, A.H.-J.; Gao, Y.-G.; Liaw, Y.-C.; Li, Y.-K. Formaldehyde Cross-Links Daunorubicin and DNA Efficiently-HPLC and X-Ray Diffraction Studies. *Biochemistry* **1991**, *30*, 3812−3815.
(58) Kelley, S. O.; Boon, E. M.; Barton, J. K.; Jackson, N. M.; Hill, M. G. Single-base mismatch detection based on charge transduction through DNA. *Nucleic Acids Res.* **1999**, *27*, 4830−4837.
(59) Gorodetsky, A. A.; Hammond, W. J.; Hill, M. G.; Slowinski, K.; Barton, J. K. Scanning Electrochemical Microscopy of DNA Monolayers Modified with Nile Blue. *Langmuir* **2008**, *24*, 14282−14288.
(60) Furst, A.; Hill, M. G.; Barton, K. A multiplexed, two-electrode platform for biosensing based on DNA-mediated charge transport. *Langmuir* **2015**, *31*, 6554−6562.
(61) Meggers, E.; Michel-Beyerle, M. E.; Giese, B. Sequence Dependent Long Range Hole Transport in DNA. *J. Am. Chem. Soc.* **1998**, *120*, 12950−12955.
(62) Giese, B.; Wessely, S.; Spormann, M.; Lindemann, U.; Meggers, E.; Michel-Beyerle, M. E. On the Mechanism of Long-Range Electron Transfer through DNA. *Angew. Chem., Int. Ed.* **1999**, *38*, 996−998.
(63) Ly, D.; Sanii, L.; Schuster, G. B. Mechanism of Charge Transport in DNA: Internally-Linked Anthraquinone Conjugates Support Phonon-Assisted Polaron Hopping. *J. Am. Chem. Soc.* **1999**, *121*, 9400−9410.
(64) Chidsey, C. E. Free energy and temperature dependence of electron transfer at the metal-electrolyte interface. *Science* **1991**, *251*, 919−922.
(65) Finklea, H. O.; Yoon, K.; Chamberlain, E.; Allen, J.; Haddox, R. Effect of the Metal on Electron Transfer acrossSelf-Assembled Monolayers. *J. Phys. Chem. B* **2001**, *105*, 3088−3092.
(66) Morris, G. P.; Simonov, A. N.; Mashkina, E. A.; Bordas, R.; Gillow, K.; Baker, R. E.; Gavaghan, D. J.; Bond, A. M. A comparison of fully automated methods of data analysis and computer assisted heuristic methods in an electrode kinetic study of the pathologically variable [Fe(CN)6](3-/4-) process by AC voltammetry. *Anal. Chem.* **2013**, *85*, 11780−11787.
(67) Lee, C.-Y.; Gong, P.; Harbers, G. M.; Grainger, D. W.; Castner, D. G.; Gamble, L. Surface Coverage and Structure of Mixed DNA/Alkylthiol Monolayers on Gold: Characterization by XPS, NEXAFS, and Fluorescence Intensity Measurements. *Anal. Chem.* **2006**, *78* (10), 3316−3325.
(68) Gong, P.; Lee, C. Y.; Gamble, L. J.; Castner, D. G.; Grainger, D. W. Hybridization behavior of mixed DNA/alkylthiol monolayers on gold: characterization by surface plasmon resonance and ^{32}P radiometric assay. *Anal. Chem.* **2006**, *78*, 3326−3334.
(69) Ellman, G. L. Tissue sulfhydryl groups. *Arch. Biochem. Biophys.* **1959**, *82*, 70−77.

https://doi.org/10.1021/jacs.1c04713
J. Am. Chem. Soc. 2021, 143, 11631−11640